

Analysis of coal combustion in oxy-fuel conditions through pulsed feeding experiments in an entrained flow reactor

C. Galletti^{1*}, E. Giacomazzi², S. Giammartini², G. Coraggio³, L. Tognotti^{1,3}

¹*Dipartimento di Ingegneria Civile e Industriale, University of Pisa, Italy*

²*ENEA – C.R. Casaccia, Rome, Italy*

³*IFRF - Livorno, Italy*

January 2013

* Corresponding author:

Dr. Chiara Galletti, Dipartimento di Ingegneria Civile ed Industriale, University of Pisa, Largo L.

Lazzarino 2, I-56126 Pisa, Italy. Tel: +39 050 2217897, Fax: +39 050 2217866, E-mail:

chiara.galletti@diccism.unipi.it

Abstract

Coal combustion is investigated in both air and oxy-fuel conditions by feeding pulses of coal particles in an entrained flow reactor able to provide high residence times. The radiant energy emitted in the range from UV to IR was collected by several photodiodes operating with high acquisition rate. The signal analysis showed the capability of the technique to capture the passage of coal streams and to identify different phenomena (e.g. volatiles ignition, char oxidation). The spatial arrangement of the photodiodes was planned in order to allow also deriving quantitative information, such as particle velocity, ignition delay and devolatilization time, from the correlation of more signals. The ignition delay was found to be higher in oxy-fuel conditions than in air, mainly because the larger specific heat of the oxy-fuel environment. The proposed diagnostics may help the qualification of advanced experimental apparatus as entrained flow reactors, with the purpose to make them suited for heterogeneous kinetics studies in oxy-fuel conditions.

Keywords: optical diagnostics; oxy-fuel combustion; ignition of coal clouds; entrained flow reactor; ignition delay.

1. Introduction

It is believed that coal will still play a fundamental role in the future for electric power production because of its low cost and abundance. Hence, large attention is paid to oxy-fuel combustion as a CO₂ capture and storage (CCS) technique for reducing greenhouse gases emission from coal plants.¹⁻

²⁻ In oxy-fuel combustion, a mixture of oxygen and recycled flue gases is used instead of air for fuel oxidation. Consequently, a gas consisting of CO₂ and H₂O is obtained, with a CO₂ concentration ready for sequestration. Flue gases are recycled in order to make up the volume of the missing N₂ and to ensure enough thermal capacity for the subsequent heat transfer operations.

In this framework, many studies in literature have been aimed at understanding solid fuel combustion in oxy-fuel conditions through the use of advanced experimental facilities able to provide data under operating conditions (i.e. temperatures and heating rates) similar to industrial ones³⁻¹⁴. Conventional analysis (e.g. thermogravimetry) on lab-scale can only give a fingerprinting of the fuel, because the thermal conditions are far from those of practical applications. For instance, pyrolysis kinetics changes substantially when varying the heating rate.

Entrained flow reactors are particularly interesting as they allow studying solid fuel combustion at high heating rates, typical of industrial ones. They are frequently used for determining solid fuel conversions in specific operating conditions; however they could potentially provide other important information (for example kinetics) but only with the aid of sophisticated experimental techniques or tedious procedures to determine the effective particle thermal history¹⁴. Indeed kinetics may strongly help the development of modelling tools (as those based on Computational Fluid Dynamics, CFD) for new combustion technologies, as most of the available models have been derived for conventional (air) combustion.

Some studies with entrained flow reactors analyse the behaviour of a single solid fuel particle, observing important features of oxy-fuel combustion. Shaddix and Molina investigated the influence of O₂/CO₂ atmosphere on the ignition of high-volatile bituminous coal and sub-bituminous coal

through single-particle imaging in an entrained flow reactor at $T = 1700$ K over a range of 12–36 % by vol. of O_2 in both N_2 and CO_2 diluent gases.³ The authors showed that the presence of CO_2 delays the onset of ignition, mainly because the higher molar specific heat of CO_2 with respect to N_2 , as well as its tendency to reduce the local radical pool. Moreover single-particle imaging demonstrated the formation of high-temperature soot clouds around the bituminous coal particles during devolatilization. Bejarano and Levendis investigated the single-particle combustion of a bituminous coal, a lignite coal and synthetic chars in both O_2/N_2 and O_2/CO_2 atmospheres (with 20–100 % by vol. of O_2) using a lab-scale drop-tube furnace operated at $T = 1400$ and 1600 K.⁴ A calibrated three-color pyrometer, interfaced with the furnace, recorded luminous particle temperature-time profiles. They showed that coal particles burned at higher mean temperatures and shorter combustion times in O_2/N_2 than in O_2/CO_2 environments at analogous oxygen mole fractions. Zhang et al.⁵ carried out an experimental investigation of the combustion of an air-dried bituminous coal in O_2/N_2 and in O_2/CO_2 atmospheres (with 21–27 % by vol. of O_2) in a lab-scale drop-tube furnace operated at $T = 1073$ and 1273 K, using an high-speed camera and two-colour pyrometer for photographic observation and particle temperature measurement. They argued that the substitution of CO_2 to N_2 affected all combustion sub-processes. Firstly, the coal pyrolysis behaviour prior ignition was enhanced, because CO_2 is reactive enough to attack the pyrolysis-driven char. Moreover the larger specific heat of CO_2 than N_2 delayed coal auto-ignition. Accordingly, a thick volatile cloud persisted on the char surface for a long duration in 21–27% O_2 in CO_2 , which caused O_2 depletion on char surface. Hence to achieve similar coal ignition intensity with in air, at least 30% O_2 in CO_2 is required. This was also confirmed by Simone et al. who used a lab-scale drop-tube reactor to analyse the conversion of an high-volatile bituminous coal at $T = 1173$ K in air and O_2/CO_2 mixtures.⁶ Jovanovic et al. evaluated coal ignition standoff length from visual observation of a Russian high-bituminous coal at $T = 1073$ – 1623 K in O_2/N_2 and O_2/CO_2 atmospheres (with 10–100 % by vol. of O_2).⁷ They showed that standoff length initially reduced significantly with increasing O_2 concentration, but for O_2 around

50% or higher the reduction was not substantial. A delayed ignition was observed for oxy-fuel conditions. Khatami et al. employed a lab-scale entrained flow reactor at $T = 1400\text{K}$ to investigate the combustion of single solid fuel particles of $d_p = 75\text{--}90\text{ }\mu\text{m}$ in O_2/N_2 and O_2/CO_2 atmospheres (with 20–100 % by vol. of O_2).⁸ Fuels included four pulverized coals from different ranks (a high-volatile bituminous, a sub-bituminous and two lignites) as well as pulverized sugarcane-bagasse. The authors found distinct combustion behaviours for the fuels, but in all cases the substitution of CO_2 to N_2 led to less intense combustion. Rathnam et al. employed an entrained flow reactor to analyse the devolatilization process of an Indonesian low-rank coal under oxy-fuel (O_2/CO_2) and air (O_2/N_2) conditions using and found that the volatile yield in CO_2 is higher than that in the N_2 atmosphere; this was attributed this to the char- CO_2 gasification reaction.⁹⁻¹⁰ Kim et al. investigated the sub-bituminous coal combustion in an entrained flow reactor using O_2/CO_2 and air O_2/N_2 atmospheres and observed a shorter flame in oxy-fuel than in the air condition.¹¹

Although the high significance and information that can be derived from such single particle studies, as a matter of fact in industrial furnaces things are more complex, as particles are fed in dense streams. Hence some recent studies have been devoted to understand the stability of oxy-coal combustion to optimise the burner design and settings.¹²

Particle group effects are likely to play a strong role for the flame-holding process in practical pulverised coal burners, where high velocity streams of particles turbulently mix with hot flame products and must ignite in tens of milliseconds.¹³ In literature there are a few studies on the combustion of dense streams of solid fuels¹⁵⁻¹⁶ and there is lack of data under oxy-fuel conditions. Du et al. proposed a model for the group ignition of a cylindrical stream of coal particles.¹⁶ They applied the model to $64\text{ }\mu\text{m}$ coal particles burning with air with different coal/air ratios (0.5, 1 and 2) and showed that homogeneous ignition occurred for dense clouds, while heterogeneous ignition for dilute ones. Moreover they observed the presence of two flames: an inner flame propagating into premixed volatiles and oxygen, and an outer diffusion flame. Recently, Liu et al. carried out

experiments on the ignition properties of two U.S. (a high-volatile bituminous and a sub-bituminous) and two Chinese (both high-volatile bituminous) coals in a laminar entrained flow reactor at $T = 1230\text{--}1320\text{ K}$ in O_2/N_2 and O_2/CO_2 atmospheres (with 12–20 % by vol. of O_2), paying attention to the coal feed rate.¹³

The coal group number was calculated for the cold feed conditions.¹³⁻¹⁵ For a cylindrical column of uniformly sized particles the group number is defined as:

$$G = \frac{3\rho_g R_c^2}{a^2 \rho_p (\dot{m}_g / \dot{m}_p)} \quad (1)$$

where ρ_g is the gas density, ρ_p is the particle density, R_c is the column radius (i.e. the feed pipe), a is the particle radius, \dot{m}_g is the mass gas flow and \dot{m}_p is the coal mass flow. It can be shown that for a given characteristic particle column radius, the group number is proportional to the product of the particle number density and the particle diameter.¹³ The group number can be easily calculated within the cold coal feed flow, but estimating it at the point of ignition is substantially more problematic, because of uncertainties regarding the expansion of the fuel jet within the reactor as a consequence of heating of the cold gas, fluid mechanical mixing, and pre-ignition devolatilization of the particles.

In the work of Liu et al., the cold flow group number, G , was varied from 0.02 to 10.¹³ The authors found that under most conditions, the ignition delay decreased with increasing coal feed rate until a minimum corresponding to a cold flow group number, G , of ~ 0.3 .

The present work describes the use of a simple optical technique (Optical Diagnostics for Combustion - ODC), based on photodiodes detecting over the UV-IR spectral range, and related analysis to derive information on solid fuel combustion in air and oxy-fuel conditions using a pilot-scale entrained flow reactor (called Isothermal Plug Flow Reactor - IPFR) thus with temperatures and heating rates similar to industrial ones. The advantage of the proposed diagnostics is the very low intrusiveness (smaller than a camera generally used in similar studies) which makes it suited for

industrial applications. The diagnostics has been successfully applied to gas combustion, especially to study thermo-acoustic instabilities¹⁷; however it is the first time that ODC is used for the characterisation of coal combustion. In particular the effect of O₂ concentration, reactor temperature, coal particle size and environment (air or oxy-fuel conditions) on coal ignition will be evaluated through the use of several ODC probes. Importantly, feeding conditions were not of a single particle, but of dense groups of particles, in order to study a situation similar to real boilers where the feed is a dense stream.

2. Experimental Section

2.1. Isothermal Plug Flow Reactor

The Isothermal Plug Flow Reactor is an entrained flow reactor, which was developed by the International Flame Research Foundation (IFRF) and is sited in the Experimental Area of ENEL Ricerca in Livorno, Italy. It allows testing solid fuels under conditions similar to industrial applications with high temperatures ($T = 1000\text{-}1600\text{ K}$) and heating rates ($10^4\text{-}10^5\text{ K/s}$).¹⁸⁻¹⁹ The reactor inner tube is 4.5 m long with a diameter of 0.15 m. At the walls, nine modules with electric resistances keep the temperature at a set point value. Each module has several ports which are available for coal injection or for the insertion of measuring instruments.

Pulverized fuel particles are transported by a carrier gas (nitrogen/air/ CO_2) and injected from a side through a radial probe (with an inner diameter of 1.4 cm and curved at the edge to allow an axial injection) into a flue gas stream and move along the reactor. Flue gases come from a pre-heating combustion section which supplies gases of desired composition and temperature. Moreover flue gases can be mixed with an additional diluent gas (such as nitrogen) to control the temperature of the gas stream. In oxy-fuel conditions, the pre-heating combustion chamber is fed with natural gas and pure oxygen, while the diluent gas is carbon dioxide in order to simulate the recycle of flue gases.

Several type B thermocouples (one for each module, i.e. nine thermocouples) are inserted in the main IPFR tube to monitor the temperature along the reactor.

At the reactor bottom, flue gas and particles are quenched down to 500 K with nitrogen and then treated in a separation and analysis system made of two cyclones and a bag filter, before being evacuated.

2.2. Operating conditions

Many operating parameters were varied to examine their effect on coal combustion.

A high volatile bituminous South African coal was used in the investigations. The ultimate and proximate analyses are given in Table 1. The coal was sieved to size ranges of $d_p = 38-90 \mu\text{m}$ and $d_p > 125 \mu\text{m}$, to evaluate the effect of the particle size on combustion.

Two IPFR temperatures were employed, i.e. $T = 1173$ and 1373 K . Both temperatures are above 1100 K that is usually considered the lowest temperature to have a fast ignition of coal streams. A preliminary characterization of the IPFR was also performed by inserting thermocouples inside the reactor fed with just flue gases, assessing that the temperature distribution inside the IPFR corresponded well to the set point temperature, the maximum observed deviation being of about 10 K .

Coal particles were entrained into mixtures with N_2 or CO_2 as diluent gases, at four different oxygen concentrations in the flue gases leaving the pre-combustion section ($Y_{\text{O}_2} = 0.5, 3, 6$ and 9% by vol.). The $Y_{\text{O}_2} = 0.5 \%$ run was aimed at analysing the behaviour in nearly absence of oxygen. The equivalence ratios, Φ , evaluated for the different experimental conditions are reported in Table 2.

The feeding of the coal particles was made in a pulsed manner: a constant volume of fuel (250 mm^3) was injected into the IPFR every 6 seconds in order to have pulses of groups of particles well separated from the others. The discharge time was about 0.5 s . At least 40 pulses for each operating condition were analysed, in order to evaluate data uncertainties. Moreover each run was repeated two or three times. The volumetric gas flow depended on temperature and oxygen fraction conditions. In fact the diluent gas (N_2 or CO_2) and air/ O_2 were fed to the pre-combustion section in order to achieve the desired composition of the flue gas streams. Flow rates used in the present investigation are given in Table 2.

The residence time of the particles in IPFR could be determined from the analysis of the signal from the ODC probes, as it will be explained in Section 3.1, and it was typically of about $\tau = 0.8 \text{ s}$ and $\tau = 1.7 \text{ s}$ for air and oxy-fuel conditions, respectively.

2.3. Optical Diagnostics of Combustion

The ODC technique was developed by ENEA (Italian Agency for Energy and Environment) to monitor combustion processes.²⁰ The ODC system is based on a photodiode which detects the radiant energy emitted by a combustion process in the spectral range from the UV to near IR (200 nm to 1100 nm). For gas combustion, such energy is the result of two effects: chemiluminescence of reactants and emission/absorption from combustion product. Hence the radiant energy emitted from the combustion process varies in time and space, as a consequence of fluctuations of the flame, stemming from the interaction between the combustion process, the turbulent eddies and the acoustic field (that has no effects in this IPFR application). Therefore, the main idea of ODC is to use the radiant energy as a non-intrusive and natural seeding to describe turbulent combustion.¹⁷ The analysis of the signal dynamics (i.e. variation with time) allows deriving important information on the flame behaviour. Indeed the ODC diodes allow operating up to very high sampling frequencies, i.e. 5 MHz. Moreover, the continuous component of the signal is compensated in order to exploit the 12 bit resolution of the DAC converter only for the dynamical part of the signal. Because of that, the signals will be reported in the graphs in “arbitrary units”, as the absolute values are of no significance. Hence, the analysis is made only on the variation of the signal. In case of coal combustion the radiant energy may come from the gaseous combustion process (volatiles oxidation), soot as well as from burning char particles.

The proposed diagnostic does not need any optical access but just a tiny nozzle. The probes are not intrusive as their upper edge is placed exactly at the reactor walls. The control volume seen from the lateral probe has a mean diameter of about 5 cm and a length equal to the IPFR diameter.

Four ODC probes were used (see Fig. 1):

- 3 probes (L1, L2, L3) were inserted from lateral ports at different distances from the coal injection (0.1265, 0.5035 and 1.003 m respectively);
- 1 probe (B1) was placed axially on the bottom of the reactor under the quench.

Consequently, lateral probes could detect fuel particles while passing in front of them, whereas the axial probe observed the fuel particles for their whole residence time in the IPFR. Such a disposition was found to be very effective as it allowed correlating different information in time and space.

The processing of signals from ODC probes was performed through sub-routines developed with the Matlab® package. Basically the signal needed the removal of the background signal due to the radiant energy emitted from the IPFR walls and flue gases coming from the pre-heating combustion section. Moreover, the absolute value of the signal is of no significance, as it depends from the stage of signal compensation performed during the signal acquisition. In addition to that, the signal noise, (due to optics and electronics) was filtered out by reporting the signal in the frequency domain through Fast Fourier Transforms (FFTs).

3. Results and Discussion

3.1. Signals description

Signals show a continuous part due to the radiant emission from the IPFR walls and flue gases from pre-heating section: every variation of the signal is caused by the passage of coal and/or the presence of a combustion process. Such a signal variation may be positive or negative depending on if the radiant energy from particles/combustion process is larger or smaller, respectively, than that coming from IPFR walls and flue gases coming from the pre-heating combustion section. Indeed, the pulsed feeding was planned on purpose to have a sufficient time lag between two successive pulses, so to discriminate the passage of a solid fuel group from flue gases.

Another aspect to consider is that bituminous coals, which have a porous structure and typically soften and swell during combustion, generate soot from heavy volatiles cracking^{3,13,21-22}. Moreover in presence of neighbouring coal particles, like is in dense clouds, soot generation is favoured.²³

An example of signal detected from lateral probes during the passage of a group of solid particles is provided in Fig. 1. As mentioned previously, signals have been pre-treated so that zero corresponds to the energy level of the reactor walls and flue gases from the pre-heating combustion section. When coal particles are injected into IPFR they are heated up until a temperature that promotes volatile ejection. A negative signal is detected if the group of coal particles emits less energy than the reactor walls and flue gases. This occurs for cold coal particles and in absence of any radiating soot. Hence for almost all cases the first probe (L1) detected a negative value of the signal while the (cold) particles were passing, as shown in Fig. 1.

The signals seen by subsequent probes (L2, L3) are affected by coal combustion behaviour, which is dependent upon oxygen fraction, reactor temperature, diluent gas as well as particle size.

For high temperatures, radiating soot and particles as well as emission from combustion products, lead to a higher radiation from the groups of particles, than from reactor walls, resulting in a positive signal. These phenomena happen when coal particles are at some distance from injection, so the L2 and L3 probes typically show a partial or total positive signal (Fig. 1).

In literature a large discussion is made about the kind of ignition a particle undergoes, i.e. homogeneous or heterogeneous ignition.²⁴ Homogeneous ignition is a two-stage process. The primary stage is the initial ignition of the volatiles; then the combustion of the volatiles is presumed to prevent char reaction by screening the solid from access by oxygen, so that secondary ignition, of the char, occurs as pyrolysis terminates. Heterogeneous ignition involves three stages: a primary stage of direct attack of the reactant gas on the coal which removes material from the solid; ignition of volatiles; eventually, re-ignition of the char at the end of pyrolysis.

In the present work, the signal analysis seems to indicate that a homogeneous ignition is occurring, because many signals seen from lateral probes, initially become negative and subsequently positive (see Fig. 1). This trend can be explained considering that a bituminous coal particle ejects heavy volatiles which initially form a spherical wake that surrounds the coal particle²², but then concentrate

behind the particle for slip and buoyant effects.²¹ The wake ignites in presence of hot oxidizing gas and a sufficient temperature; moreover it is known that during this stage the wake has a temperature much higher than the solid particle.³ Hence, soot and wake of ignited volatiles have a temperature much higher than ambient (reactor walls and flue gases), while the solid char particles still have a temperature colder than the ambient one. The above observation is valid for single particles, but it is probably reproducible for group of particles, like in this study, and thus explaining the kind of signal (i.e. negative and subsequently positive) observed by the lateral probes, as well as their variation with operating conditions. However further investigation is needed to better corroborate this hypothesis. Also Khatami et al. observed homogeneous ignition (which they denoted as two-mode combustion) for a bituminous coal particle fed with 21-37% O₂ in N₂.⁸

As a matter of fact, for the dense coal cloud conditions of the present work, the wake is formed by volatiles ejected from many particles, but volatiles ignite in an only one big flame as indicated by the large group numbers.²³

The group number was calculated for the cold feed conditions.¹³⁻¹⁵ For a cylindrical column of uniformly sized particles the group number is defined as:

$$G = \frac{3\rho_g R_c^2}{a^2 \rho_p (\dot{m}_g / \dot{m}_p)} \quad (1)$$

where ρ_g is the gas density, ρ_p is the particle density, R_c is the column radius (i.e. the feed pipe), a is the particle radius, \dot{m}_g is the mass gas flow and \dot{m}_p is the coal mass flow. For the pulsed injections and for the $d_p > 125 \mu\text{m}$ particles the group number was about $G = 9.7$, while for $d_p = 38-90 \mu\text{m}$ particles the group number was $G = 40.1$. Such group numbers allow investigating conditions similar to industrial furnaces. For instance simulations in a semi-industrial furnace equipped with an aerodynamically air-staged burner indicated that the group number in the zone where ignition takes place is around 40 with fuel/air ratios of about 0.13.²⁵

An example of signal detected from the probe placed in the bottom of the reactor (B1) is given in Fig. 2 along with camera images taken from the bottom of the reactor. It is worth observing that this probe can see all the process. There is a first attenuation of the signal corresponding to the injection of cold coal particles, which are then heated up. Subsequently, the signal increases quickly up to a maximum, because of the luminous emission from volatiles oxidation, and subsequently decreases because volatiles are consumed. Then the high signal plateau corresponds to char oxidation. This behaviour is consistent with homogeneous ignition. Subsequently, the quench leads to a very sharp decrease of the signal towards very negative values, also because particles are more concentrated in the sampling probe.

Therefore the B1 probe allow evaluating the particle residence time in the reactor as the time interval between the first signal attenuation (corresponding to the injection of coal particle) and the end of the negative signal (corresponding to the exit of coal particles from the reactor after the quench). For instance Fig. 2 indicates a residence time of about 1.6 s.

3.2. Effect of the O_2 fraction

The oxygen fraction does not affect strongly the devolatilization process, but has an important effect on the volatiles ignition. The diffusion of oxygen from the bulk of the gas to the coal particle surface increases with increasing the oxygen gradient, according to the Fick's law. The ejected volatiles, on the contrary, diffuse from the coal particle surface toward the bulk of the gas, so that a higher oxygen concentration causes a faster ignition of the wake of volatiles.

This effect may be observed from the signals from lateral probes where the occurrence of the first positive signals (related to volatiles oxidation) is anticipated with increasing O_2 fraction. Also the B1 probe signal confirmed that. Three considerations on the effect of increasing Y_{O_2} may be derived from Fig. 3a, which shows the signals from the bottom probe for $T = 1373$ K and N_2 diluent: increasing Y_{O_2} the signal increases with a larger slope, the intensity of the first peak increases, the difference between first peak (volatile ignition) and the signal of char oxidation increases. All these

considerations are consistent with the theory that volatile oxidation is faster and more intense if the oxygen concentration is higher.

3.3. Effect of the reactor temperature

Temperature affects many aspects of coal combustion. An increase of temperature may lead to higher heating rates, faster devolatilization, faster volatile oxidation and faster char combustion. The latter aspect cannot be fully analysed because the residence time of char particles in the IPFR was not high enough to complete char oxidation before the quench. Fig. 4 shows signals from lateral probes at different reactor temperatures. The signals for $T = 1173$ K and 1373 K are completely different. At $T = 1173$ K (Fig. 4a) the signal of the first probe is almost entirely negative, whereas the second probe shows both a negative and a positive part. Conversely, for $T = 1373$ K (Fig. 4b) the first probe detects both a positive and negative signal, whereas the second probe shows a fully positive signal. Therefore volatiles ignition occurred as the coal reached the first probe location for $T = 1373$ K, whereas it was just started at the second probe position for $T = 1173$ K.

3.4. Effect of particle size

For single particles, it is known that smaller particles are subjected to a faster heating rate and have a lower flame temperature than larger ones.⁴ However the group number of Eq. (1) should be taken into account when comparing different particle sizes. In particular a larger group number causes a lower heating rate. The group number for smaller particles was $G = 40.1$, much higher than for larger particles ($G = 9.7$); thus the effect of the group number on the heating rate is opposite to the effect of particle size. Moreover the shape of the feeding jet should be considered when comparing different coal particle size. In particular, preliminary CFD simulations have shown that larger particles spread more towards the reactor walls because of to the feeding probe geometry.²⁶ The signals from lateral probes showed not significant differences in the ignition for the different particle sizes. Actually we should consider that the probes allow only a discretized vision of the space; in

other words probably more probes should be fitted within the same distance to capture small differences in the ignition behaviour. Instead, the signals from B1 probe (this is the probe that is able to capture all the process) showed clearly that for the largest particles the intensity of the first peak in the signal is very high and well distinct from the plateau corresponding to char oxidation (see Fig. 6). Such a difference was less evident for the smallest particles. This means that for the largest size investigated there is a well separation of the volatiles oxidation and soot emission from the following char combustion. Indeed, the signals from the largest particles showed a primary homogeneous ignition and a subsequently secondary char oxidation, while in the smallest particles the two phenomena partially overlapped in the final part of volatiles oxidation. Thus the ignition of char occurred earlier for smallest particles than for the largest ones. This aspect is in accordance with the fact that heterogeneous ignition is more likely to occur for small particles size. Indeed Howard and Essenhigh indicated that there is a critical particle size, below which the volatiles matter does not lift from the particle surface and thus volatiles and chars burn simultaneously or near the particle surface.²⁷

3.5. Effect of diluent gas

The effect of the diluent gas (N_2 and CO_2) was evaluated at the same reactor temperature ($T = 1373$ K) and for the same particle size ($d_p = 38-90 \mu m$). As mentioned in the introduction, the available studies in literature show that oxy-fuel combustion (in CO_2 atmosphere) is slower than combustion in N_2 , especially because of the larger heat capacity of CO_2 , that makes volatiles combustion occurring in an ambient at lower local temperature.^{3,8} This agrees with signals from lateral probes, showing that in case of CO_2 atmosphere positive signals (i.e. emission) occurred at larger distances from the injections than for N_2 atmosphere. Moreover it is known that in presence of O_2 , volatiles do not ignite in CO_2 atmosphere as soon as in N_2 atmosphere, but stay unburned around the solid particle for some time.⁹ This is probably due to the lower molecular diffusivity of both oxygen and

volatiles in CO₂ than in N₂ atmosphere, which prevents the mixing of reactants, as well as to the higher ignition temperature in CO₂ atmosphere.⁸

Fig. 3b shows the effect of different O₂ concentration in case of CO₂ diluent. At higher O₂ fractions there is a large difference between the intensity of the first peak and the signal corresponding to char oxidation, as also observed in Fig. 3a in case of N₂ as diluent gas.

3.6. Ignition delay analysis

The ignition delay of the coal particles' clouds for all the conditions tested was evaluated by relating the lateral and the bottom probes' signals. The ignition delay was calculated as the time interval between coal injection and the time at which the signal seen by the bottom probe starts to increase considerably. This latter condition represents a state of initial ignition that can be related to volatile oxidation and could be easily determined from the signal analysis. Coal injection was not directly determined because the fed coal particles are too little and too far from the bottom probe (placed about 4 m above the coal injection) to cause an important decrease of the signal. So the injection time was determined with the aid of the first lateral probe. This probe was placed only 0.1265 m below of the coal injection point, thus it could reveal the passage of a group of (cold) solid particles through a well decrease of the signal. Particles were injected with a velocity of around 9.3 m/s; however it should be considered the jet decay when evaluating the particle velocity at downstream positions. As a matter of fact, the particle velocity may be estimated by the comparison of signals taken at the different lateral ports. In particular it was evaluated a particle velocity of about 6.1 m/s between the first lateral probe (i.e., L1, placed 0.1265 m below coal injection) and the second one (i.e., L2, placed 0.503 m below coal injection). Subsequently it was assumed that particles flowed with a medium velocity of about 8 m/s between the coal injection and the first lateral probe. With this hypothesis the time between coal injection and the transit of the first coal particles in front of the first probe was evaluated to be of about 16 ms, from the ratio between the distance from injection to

first probe and the mean velocity. Therefore the coal injection time could be determined by subtracting 16 ms from the time the particles started to be seen by the first lateral probe.

Ignition delay results as well as relative errors (evaluated from the standard deviation of data take) are reported in Fig. 5 for the $d_p = 38\text{-}90\text{ }\mu\text{m}$. The errors represent the standard deviation of the dataset of ignition delays evaluated from all (at least 40) solid fuel pulses.

Fig. 5 shows the strong effect of reactor temperature on ignition delay at different Y_{O_2} for N_2 diluent and basically confirms observations made in Section 3.3.

As far as the effect of O_2 fraction is concerned, the ignition delay decreases with increasing the O_2 fraction (thus with increasing the reactivity of the volatiles-oxidiser mixture). For instance at $T = 1373\text{ K}$ the ignition time decreases from 77 to 65 ms with increasing for Y_{O_2} from 6 to 9%. The observed trend is in agreement with other works in literature.^{3-4,7.}

Also in oxy-fuel conditions it was observed a decrease of ignition delay time with the increase of the oxygen fraction (see Fig. 7a). Moreover, larger ignition delay times were observed in oxy-fuel conditions (CO_2 diluent) than in air condition (N_2 diluent), in agreement with the work of Shaddix and Molina.³ This may be imputed to the higher heat capacity of CO_2 with respect to N_2 . It can be shown from the adiabatic thermal explosion theory for a one-step overall reaction that the auto-ignition time increases linearly with the specific heat according to the following equation³:

$$\tau_i = \frac{c_v (T_0^2 / T_a)}{q_c Y_{F,0} A \exp(-T_0^2 / T_a)} \quad (2)$$

where c_v is the specific heat at constant volume, T_0 is the initial temperature of the fuel/oxidiser mixture, q_c is the combustion heat release per mass of fuel, $Y_{F,0}$ is the initial mass fraction of the fuel and the reactivity of the fuel/oxidiser mixture is given by $k = A \exp(-T_a / T_0)$, in which T_a represents the activation temperature.

In oxy-fuel conditions, a possible source of influence on the ignition delay time may be related to the production of radicals via thermal dissociation of CO_2 ; however this reaction is negligible at the temperature of the present experiments.³ CO_2 may also effect ignition delay by reducing the rate of primary CO oxidation reaction (i.e. $\text{CO} + \text{OH} \leftrightarrow \text{CO}_2 + \text{H}$) and enhancing key recombination reactions (e.g. $\text{H} + \text{O}_2 + \text{M} \leftrightarrow \text{HO}_2 + \text{M}^{28}$).³

Fig. 7b shows the ignition time to molar specific heat ratio, τ_i/c_v , for both air and oxy-fuel conditions. The molar specific heat has been evaluated at 1373 K for O_2/N_2 and O_2/CO_2 mixtures. It can be noticed only minor differences (of the order of the uncertainty) between air and oxy-fuel conditions, thus confirming that the main reason for higher ignition delay in CO_2 atmosphere is due to the higher heat capacity of CO_2 . It should be noticed that the present values of ignition delay are higher than those reported in other works³, however this may be partly imputed to the different coal tested, different operating conditions as well as the different (i.e. higher) particle numerical density. For instance ignition delay times of 5-12 ms were observed by Shaddix and Molina³, but for much higher oxygen concentration and temperature ($T = 1700$ K) and for a single particle. Actually our high particle density was aimed at investigating fuel/gas carrier ratios not far from the typical fuel/air ratios of real boilers, thus for conditions of large group numbers.

4. Conclusions

A simple technique, based on photodiodes detecting in the UV-IR range, has been applied to a pilot-scale entrained flow reactor, characterised by high particle residence times, in order to gain insight on coal combustion in air and oxy-fuel conditions. The feeding of the particles was made in a pulsed manner in order to have well identified groups of solid fuel particles. Particles were fed in dense conditions; the group number was typical of group combustion, being 9.7 for large particle and 40.1 for smaller particles. The technique was found to be able to capture the passage of coal streams and to identify different phenomena (e.g. volatiles ignition, char oxidation). Signals from several probes

were correlated in order to derive quantitative information, such as particle velocity, ignition delay and devolatilization time. The signals were found to be sensitive to operating conditions, such as O₂ concentration, reactor temperature, and environment as well particle size. In particular increasing O₂ concentration and/or reactor temperature anticipates the volatiles ignition. It was found that the ignition delay is higher in oxy-fuel conditions than in air conditions, mainly because the higher heat capacity of O₂/CO₂ mixtures than O₂/N₂ mixtures, thus confirming results obtained in literature also for single particle studies³.

The data that can be derived from such technique may help the determination of kinetics from entrained flow reactors, without the need of sophisticated diagnostics. All this information is very valuable for the validation of heterogeneous combustion sub-model to be coupled with Computational Fluid Dynamics.^{29,30}

Results are encouraging, especially because the low intrusiveness of the probe suggests its use for industrial applications. Therefore IFRF and ENEA are actually performing experimental campaigns on a 3 MW semi-industrial furnace burning coal in oxy-fuel conditions.

Acknowledgments

We would like to thank Ing. Stefano Tarquini, who was actively involved in the analysis of experimental data.

References

- (1) Wall, T.; Liu, Y.; Spero, C.; Elliot, L.; Khare, S.; Rathnam, R.; Zeenathal, F.; Moghtaderi, B.; Buhre, B.; Sheng, C.; Gupta, R.; Yamada, T.; Makino, K.; Yu, J. *Chem. Eng. Res. Des.* **2009**, *87*, 1003-1016.
- (2) Chen, L.; Yong, S. Z.; Ghoniem, F. *Progr. Energy. Comb. Sci.* **2012**, *38*, 156-214.
- (3) Shaddix, C. R.; Molina, S. *Proc. Combust. Inst.* **2009**, *32*, 2091-2098.
- (4) Bejarano, P. A.; Levendis, Y. A. *Comb. Flame* **2008**, *153*, 270-287.
- (5) Zhang, L.; Binner, E.; Qiao, Y.; Li, C. Z. *Fuel* **2010**, *89*, 2703-2712.
- (6) Simone, M.; Marcucci, M.; Biagini, E.; Galletti, C.; Tognotti, L. *Chem. Eng. Trans.* **2009**, *17*, 181-186.
- (7) Jovanovic, R.; Milewska, A.; Swiatkowski, B.; Goanta, A.; Spliethoff, H. *Int. J. Heat Mass Transfer* **2011**, *54*, 921-931.
- (8) Khatami, R.; Stievers, C.; Joshi, Y.K.; Levendis, A.; Sarofim, A.F. *Comb. Flame* **2012**, *159*, 1253–1271.
- (9) Rathnam, R. K.; Elliott, L.K.; Wall, T.F.; Liu, Y.; Moghtaderi, B. *Fuel Proc. Technol.* **2009**, *90*, 797-802.
- (10) Li, X. C.; Rathnam, R. K.; Yu, J. L.; Wang, Q.; Wall, T.; Meesri, C. *Energy Fuels* **2010**, *24*, 160-164.
- (11) Kim, Y.-G.; Kim J.-D.; Lee, B.-H.; Song, J.-H., Chang, Y.-J; Jeon, C.-H. *Energy Fuels* **2010**, *24*, 6034–6040.
- (12) Khare, S.P.; Wall, T.F.; Farida, A.Z.; Liu, Y.; Moghtaderi, B.; Gupta, R. P. *Fuel* **2008**, *87*, 1042-1049.
- (13) Liu, Y.; Geier, M.; Molina, A.; Shaddix, C. R. *Int J Greenhouse Gas Control* **2011**, *55*, 536-546.
- (14) Simone, M.; Biagini, E.; Galletti, C.; Tognotti, L. *Fuel* **2009**, *88*, 1818–1827

- (15) Ruiz, M.; Annamalai, K.; Dahdah, K.; in: Grosshandler WL, Semerjian HG (Eds), ASME HTD-Vol. 148, *Heat and mass transfer in fires and combustion systems*, **1990**, p. 16-26.
- (16) Du , X.; Gopalakrishnan, C.; Annamalai, K. *Fuel* **1995**, 74, 487-494.
- (17) Bruschi, R.; Giacomazzi, E.; Giammartini, S.; Giulietti, E.; Manfredi, F.; Stringola, C.; Daniele, S.; AIAA-2005-4328, *41st AIAA/ASME/SAE/ASEE Joint Propulsion Conference & Exhibit* **2005**, Tucson, Arizona, USA.
- (18) Biagini, E.; Biasci, L.; Marcucci, M.; *Description of the Isothermal Plug Flow Reactor and experimental procedures for combustion studies on solid fuels*, IFRF Report No. G03/y/03, International Flame Research Foundation, **2010**.
- (19) Karlström, O.; Brink, A.; Hupa, M.; Tognotti, L. *Comb. Flame* **2011**, 158, 2056-2063.
- (20) Giacomazzi, E.; Troiani, G.; Giulietti, E.; Bruschi, E. *Exp. Fluids* **2008**, 44, 557-564.
- (21) Levendis, Y. A.; Joshi, K.; Khatami, R.; Sarofim, A.F. *Comb. Flame* **2011**, 158, 452-465.
- (22) McLean, W.J.; Hardesty, D.R.; Pohl, J.H. *Proc. Combust. Inst.* **1981**, 18, 1239-1248.
- (23) Annamalai, K.; Ryan, W.; Dhanapalan, S. *Prog. Energy Combust. Sci* **1994**, 20, 487-618.
- (24) Essenhigh, R.H.; Misra, M.; Shaw, D. *Comb. Flame* **1989**, 77, 3-30.
- (25) Galletti, C.; Coraggio, G., Tognotti, L. (2012). *Modeling oxy-coal combustion in a semi-industrial furnace*. In: 17th Members' Conference. International Flame Research Foundation, **2012**, Paris. ISBN: 978-88-908091-0-1.
- (26) Galletti, C.; Tarquini, S; Bruschi, R.; Giammartini, S.; Coraggio, G.; Tognotti, L. *Ignition delay of coal particle clouds in oxy-fuel conditions*. In: 17th Members' Conference. International Flame Research Foundation, **2012**, Paris. ISBN: 978-88-908091-0-1.
- (27) Howard, J. B.; Essenhigh, R. H., *Proc. Comb. Inst* **1967**, 11, 399-408.
- (28) Davis, S.G.; Joshi, A.V.; Wang, H.; Egolfopoulos, F. *Proc. Comb. Inst* **2005**, 30, 1283-1292.
- (29) Jovanovic, R.; Milewska, A.; Swiatkowski B., Goanta, A.; Spliethoff, H. *Fuel* **2012**, 101, 23-37.

- (30) Galletti, C.; Coraggio, G., Tognotti, L. *Fuel* **2013**, in press. DOI: 10.1016/j.fuel.2013.02.061.

Table 1 – Proximate analysis of bituminous South African Coal.

d_p [μm]	<i>Moisture</i> [% wet]	<i>VM</i> [% wet]	<i>FC</i> [% wet]	<i>Ash</i> [% dry]	<i>C</i> [% dry]	<i>H</i> [% dry]	<i>N</i> [% dry]	<i>O</i> [% dry]
38-90	2.37	28.01	53.45	16.55	68.10	4.10	1.53	9.72
125	2.97	28.02	55.60	13.82	69.43	4.44	1.63	10.68

Table 2 – List of all experimental conditions.

			flow rates in the pre-heating combustion section				carrier flow rate		flue gases composition (measurements)			
d_p [μm]	T [K]	nominal Y_{O_2} [% dry]	F_{GN} [Nm ³ /h]	F_{AIR} [Nm ³ /h]	F_{O_2} [Nm ³ /h]	F_{CO_2} [Nm ³ /h]	F_{N_2} [Nm ³ /h]	F_{AIR} [Nm ³ /h]	CO_2 [% vol]	CO [ppm]	O_2 [% vol]	Φ [-]
38-90	1173	0	2.24	22.6			1.2		8.5	0.24	0.7	
		3	2.29	27.3			1.2		7.2	0.15	3.15	1.40
		6	2.19	30.3			1.2		7.6	0.13	6.31	0.75
	1373	0.5	2.17	21.5			1.2		10.1	1.06	0.41	10.8
		3	2.17	24.9			1.2		8.8	0.26	3.05	1.75
		6	2.17	30			1.2		7.5	0.21	5.96	0.74
		9	2.17	35.8			1.2		6.9	0.15	9.15	0.47
		0	1.69		3.65	9	1.2		+	3.02	0.81	8.64
		3	1.69		3.95	9	1.2		+	2.2	3.7	2.58
		6	1.69		4.3	9	1.2		+	2.12	6.63	2.13
		9	1.69		4.75	9	1.2		+	2.2	9.45	0.66
	>125	0	2.19	21.4			1.2		11.6	0.31	0.54	
		3	2.19	24.8			1.2		9.3	0.16	3.2	1.86
		6	2.19	30.3			1.2		7.8	0.08	6.32	0.75
		0.5	2.17	21.4			0.6	0.6	10	0.53	0.73	6.37
		3	2.14	24.9			1.2		8.7	0.25	3.12	1.78
		6	2.14	29.8			1.2		7.5	0.21	5.99	0.76
		9	2.14	35.4			1.2		6.9	0.17	9.09	0.48

+ = measurements could not be performed as above the upper threshold of the instrument.

Figure Captions

Fig. 1 - Scheme of IPFR, arrangement and signals of L1, L2, L3 and B1 ODC probes.

Fig. 2 - Example of signal from the bottom probe and related images from a bottom camera.

Fig. 3 - Signals detected from B1 probe for different O₂ concentration with (a) N₂ and (b) CO₂ diluent gas. $T = 1373 \text{ K}$, $\delta\pi = 38\text{-}90 \text{ }\mu\text{m}$.

Fig. 4 - Signals detected from L1 and L2 probes for different reactor temperatures: (a) $T = 1173 \text{ K}$ and (b) $T = 1373 \text{ K}$.

Fig. 5 - Ignition delay as a function of the O₂ fraction for different reactor temperatures. N₂ diluent

Fig. 6- Signals detected from B1 probe for different particle size: (a) $d_p = 38\text{-}90 \text{ }\mu\text{m}$; (a) $d_p > 125 \text{ }\mu\text{m}$. $T = 1173 \text{ K}$, $Y_{O_2} = 3\%$, N_2 diluent.

Fig. 7 – (a) Ignition delay and (b) ignition delay to specific heat ratio as a function of O₂ fraction for different diluent gases. $T = 1373 \text{ K}$, $d_p = 38\text{-}90 \text{ }\mu\text{m}$.

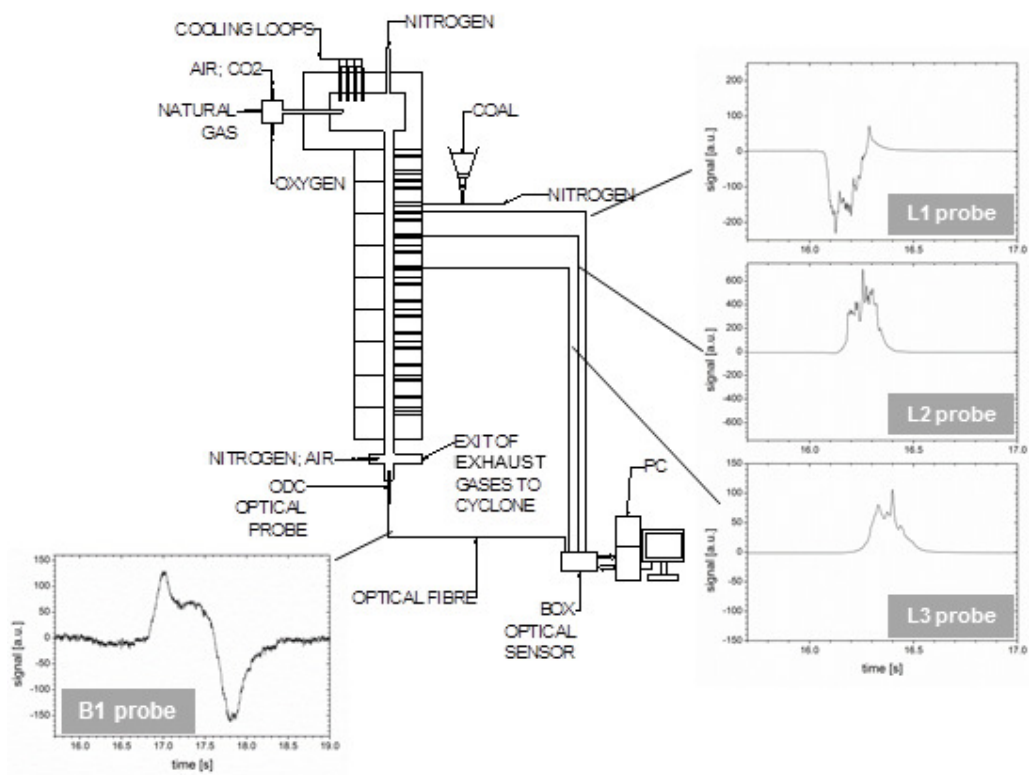


Fig. 1 - Scheme of IPFR, arrangement and signals of L1, L2, L3 and B1 ODC probes.

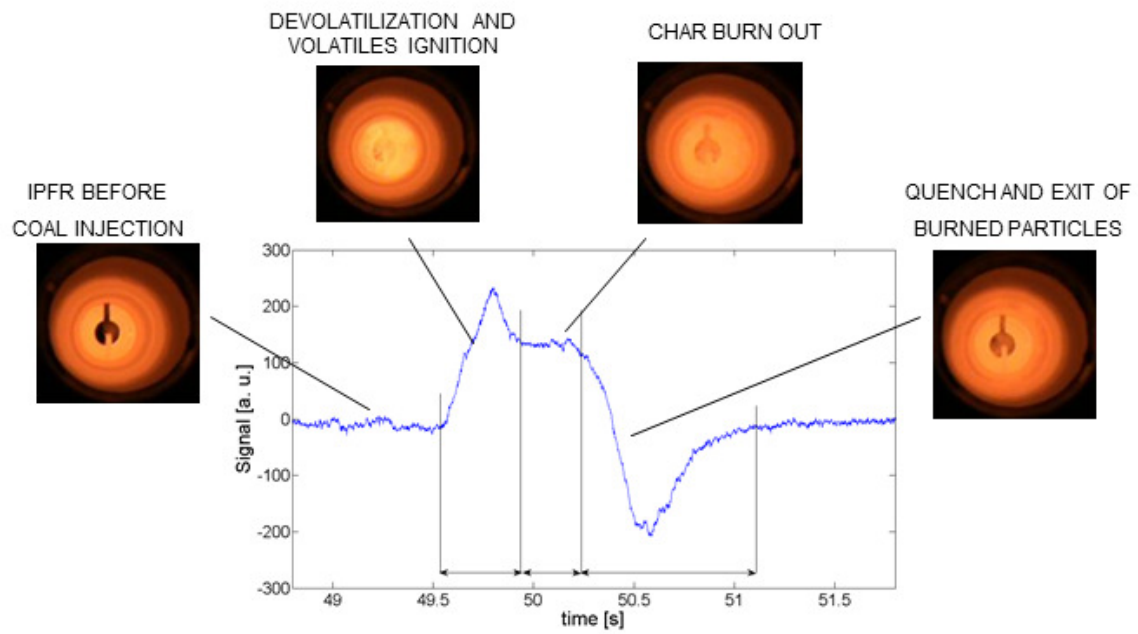


Fig. 2 - Example of signal from the bottom probe and related images from a bottom camera.

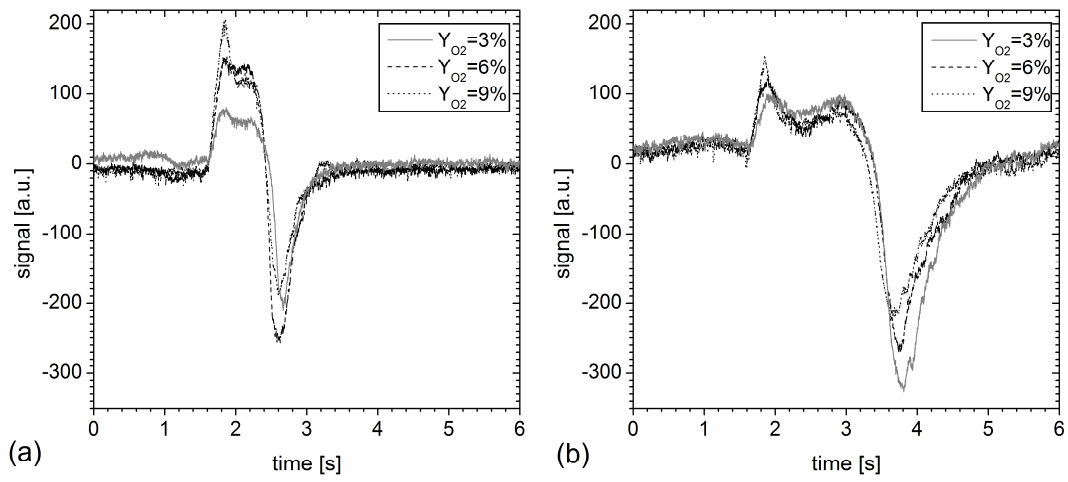


Fig. 3 - Signals detected from B1 probe for different O_2 concentration with (a) N_2 and (b) CO_2 diluent gas. $T = 1373$ K, $d_p = 38\text{-}90$ μm .

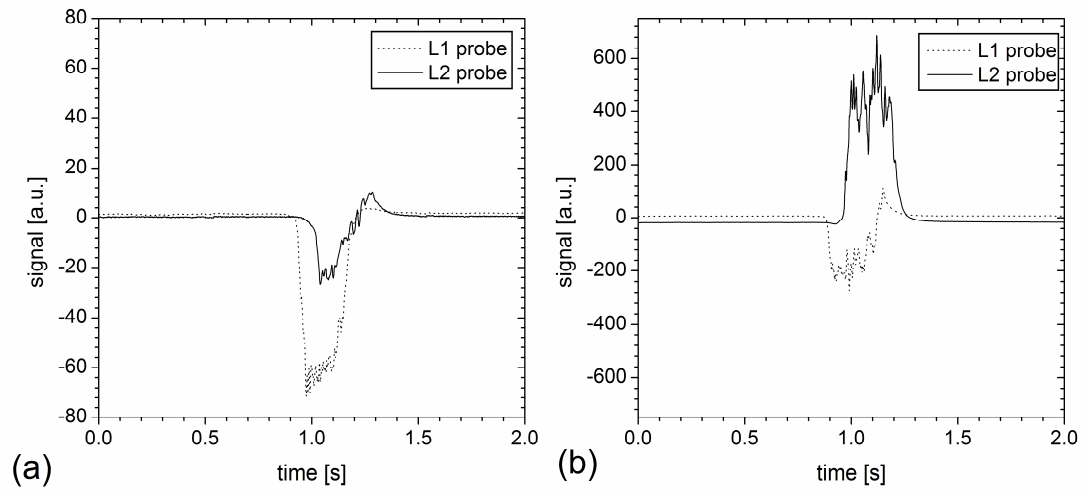


Fig. 4 - Signals detected from L1 and L2 probes for different reactor temperatures: (a) $T = 1173$ K and (b) $T = 1373$ K. $d_p = 38\text{-}90\text{ }\mu\text{m}$.

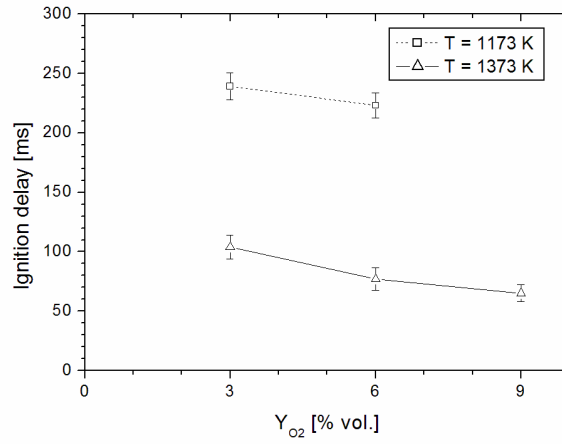


Fig. 5 - Ignition delay as a function of the O_2 fraction for different reactor temperatures. N_2 diluent gas, $d_p = 38\text{-}90\text{ }\mu\text{m}$.

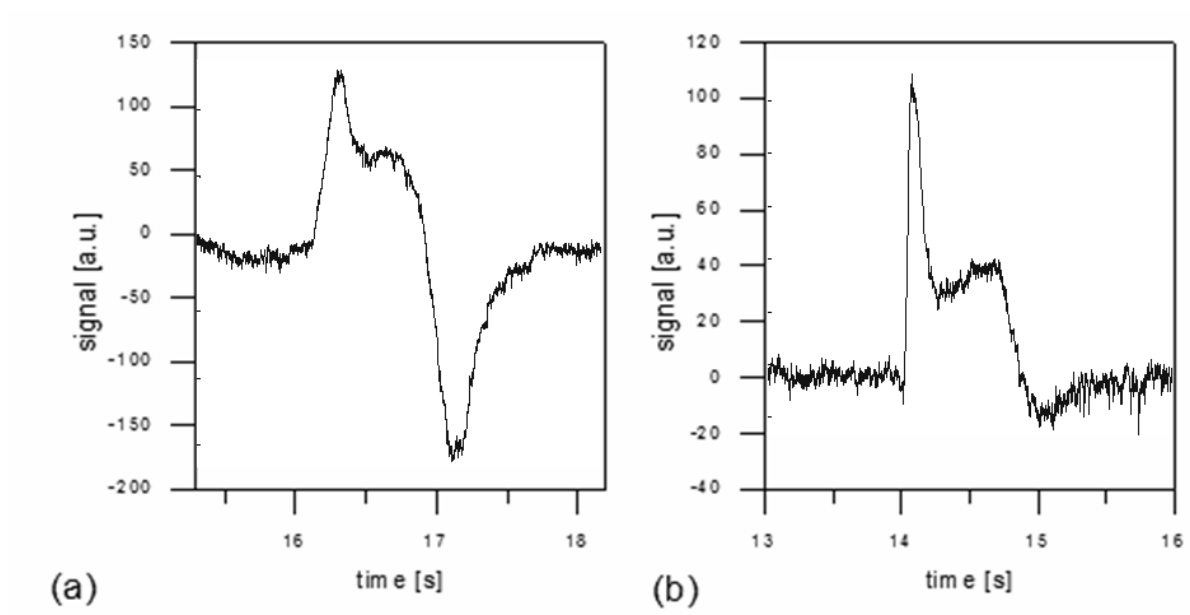


Fig. 6- Signals detected from B1 probe for different particle size: (a) $d_p = 38-90 \mu\text{m}$; (a) $d_p > 125 \mu\text{m}$. $T = 1173 \text{ K}$, $Y_{O_2} = 3\%$, N_2 diluent.

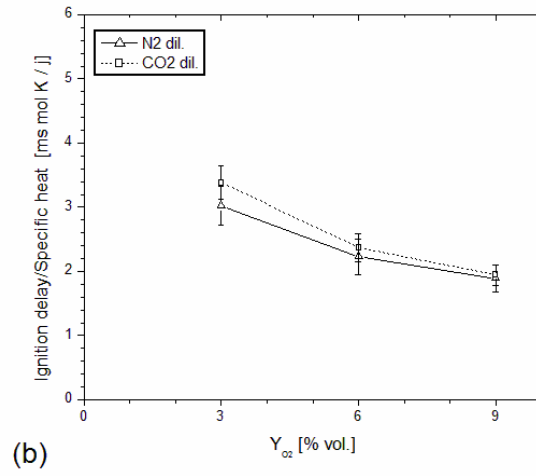
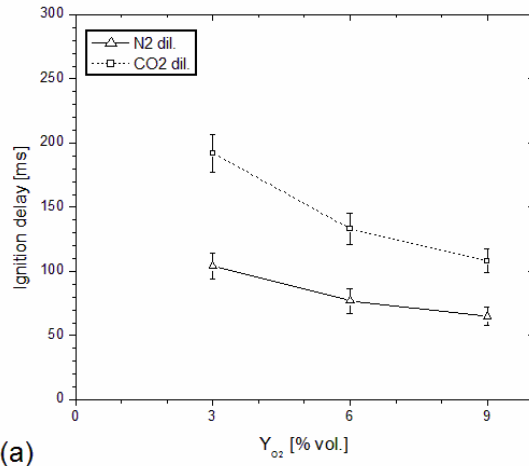


Fig. 7 – (a) Ignition delay and (b) ignition delay to specific heat ratio as a function of O_2 fraction for different diluent gases. $T = 1373\text{ K}$, $d_p = 38\text{-}90\text{ }\mu\text{m}$.